The critical role of newly green corrosion inhibitors shows the disruption of cathodic and anodic reactions at the metals and solution interface. The object of this study is the development of Saga as a corrosion inhibitor to mitigate the effect of corrosive HCl 1M on mild steel. The inhibitor was extracted using methanol to prepare various concentrations. Fourier transform infrared (FTIR) spectroscopy was used to determine the functional group of the inhibitor. The electrochemical impedance spectroscopy aided by the potentiodynamic polarization was utilized to evaluate the inhibitor's effectiveness. Optical emission spectroscopy (OES) was implemented to determine the percentage of elements in mild steel. Based on the FTIR results, C=O, -OH, C=C, benzene, and C-O are accountable for the inhibitor to donate its lone pair of an electron to the 3-d orbital of iron metal. Increasing the inhibitor concentration decreases the capacitive double layer to elevate the inhibitor resistance. The higher inhibitor resistance of 29.33 Ω cm^{-1} increases as the concentration increases due to the depression of Cdl 420.16 μF cm^2 at 10 ml inhibitor solution. Parallelly, it increases the inhibition efficiency at 65.58 %, slightly lower than the PP measurement of nearly 88 %. The higher value of adsorption/desorption constant, Kads, at 2.9 L mol^{-1} shows the strength of the inhibitor, which lowers the value of Gibbs free energy (ΔGads). The Saga inhibitor is considered a chemisorption inhibitor ΔGads −36.87 kJ/mol. The value demonstrates the formation of dative covalent bonding, which promotes the transferred electron from the inhibitor to the substrate. On the other hand, the Saga inhibitor abides by the Langmuir adsorption isotherm as the R^2 value is 0.99

Keywords: Saga inhibitor, green corrosion inhibitor, Langmuir adsorption isotherm, chemisorption

UDC 620
DOI: 10.15587/1729-4061.2022.263236

DEVELOPMENT OF SAGA (ABRUS PRECATORIUS) SEED EXTRACT AS A GREEN CORROSION INHIBITOR IN API 5L GRADE B UNDER 1M HCL SOLUTIONS

Rini Riastuti
Corresponding Author
Doctor of Engineering, Senior Lecturer*
E-mail: riastuti@metal.ui.ac.id
Dinar Setiawidiani
Master of Engineering*
Johny Wahyuadi Soedarsono
Doctor of Engineering, Professor**
Sidhi Aribowo
Master of Science, Senior Engineer*
Agus Paul Setiawan Kaban
Master of Engineering, Doctoral degree Student*
*Prof Johny Wahyuadi Laboratory**
**Department of Metallurgical and Materials Engineering
Universitas Indonesia
Kampus Baru UI Depok, Jawa Barat, Indonesia, 16424

Received date 15.06.2022
Accepted date 09.08.2022
Published date 31.08.2022

***How to Cite**: Riastuti, R., Setiawidiani, D., J. Soedarsono, W., Aribowo, S., Kaban, A. P. S. (2022). Development of saga (abrusprecatorius) seed extract as a green corrosion inhibitor in API 5L Grade B under 1M HCL solutions. Eastern-European Journal of Enterprise Technologies, 4 (8 (118)), 46–56. doi: https://doi.org/10.15587/1729-4061.2022.263236*

1. Introduction

In the modern world, timed delivery of oil and gas is crucial to ensure the smoothness of industrial and engineering processes. It is important to note that the role of pipelines is indisputable to safely and efficiently transport hydrocarbon. The standard material to compose the pipelines is carbon steel (CS), which is broadly utilized in oil and gas companies and other industries due to its superior mechanical strength, thermal conductivity, and affordable price [1]. However, the impurities such as CO_2 gas and the acidic conditioning fluid of the inner layer of pipelines increase the risk of failure due to corrosion [2–5]. By default, corrosion is an electrochemical reaction between the corrosive substance and the metal, progressing to metal deterioration without strict prevention.

Introducing a green corrosion inhibitor (GCI) [6] is one of the greenest solutions for corrosion mitigation in modern society to inhibit the corrosion effect in CS while keeping the disposal of inhibitor remains at a safety level. Before the inhibitor introduction period, the productivity of CS may be lowered and unprotected to secure the integrity of pipelines due to corrosion threats from corrosive substances such as lower pH fluid in the pipelines.

As a result, adding GCI is considered to be an excellent practice to depress the unexpected pipeline's failure (e.g. wall thinning) and remains critical to protecting the metal surface. In addition, the research on utilizing natural plants as GCI has significantly developed, including their pre-processing inhibitor extraction and their compatibility in various environmental conditions.

Several previous works have been developed to earn the benefit of using natural resources as a means to reduce the impact of corrosion. The study [7] harnesses the potential of *Morinda Citrifolia* to induce the chemical bonding between

the inhibitor and CS under artificial seawater. Under the same corrosive medium, the research [8] shows the *Secang* heartwood extract was used as a corrosion inhibitor with lower inhibition efficiency of 53.18 %. On the other hand, the study [9] provides information about the role of *Eleutherine Americana Merr. Extract* as a corrosion inhibitor to control the electrochemical activity on API 5L X42 under low pH of HCl. The previous works demonstrate that GCI is the solution to address the toxicity issue of the existing inorganic corrosion inhibitor. Furthermore, white tea [10] and rice husk ash [11] have been used to protect the steel in an acidic environment with lower toxicity and high thermal resistance.

The existing research continues to elaborate on the potential of *Abrus precatorius* (AP) or Saga as a natural inhibitor. The study [12] has recently paved the way to elaborate on the AP inhibitor on aluminum under alkaline conditions. However, the limitation of the published work shows its inadequacies in explaining the inhibition mechanism of the AP when the CS is submerged under acidic conditions. The reduction of electrochemical activity of the inhibitive mechanism includes the interaction between the significant role of oxygen and the benzene functional group of the inhibitor on the surface of metals.

As a result of this study, a practical guideline is given since the engineer or researcher may benefit from gaining information of the actual inhibitor dosage [13] to protect the substrate (CS) fully. The higher inhibitor dosage may require a higher cost to provide the inhibitor. Therefore, the recommendation of the actual cost may depress the maintenance and operational cost of the company. Thus, devoted studies are related to determining the inhibition efficiency of the inhibitor to protect the CS from corrosion. At the same time, this enables the research to be relevant to show AP's performance and mechanism of inhibition under a low pH solution.

2. Literature review and problem statement

Corrosion inhibitor is inseparable from the rapid utilization of the acidic solutions used in the industry, which generally causes damage on the surface of materials through electrochemical reaction [14]. The lower pH solution improves the production of the oil well, although the overuse of acidic solutions causes greater business loss due to corrosion. Therefore, the strategic plan to reduce the effect of corrosion is critical. One affordable and effective instrument to depress corrosion is the introduction of a green corrosion inhibitor from plant material. A previous study [15] shows piper betle and green tea as an inhibitor to modify the redox reaction of API 5L X-42 metal under a 3.5 % NaCl solution.

However, the study retains unresolved work related to the green inhibitor concept. The paper [16] shows that most organic corrosion inhibitors are vastly harmless and should exhibit a value of partition coefficient less than 3. Less toxic inhibitor demonstrates high solubility in water by having a shorter period to be fully dissociated and being accepted to degrade in the environment. Hence, the challenges of discovering an eco-friendly inhibitor have grown rapidly in recent times. On the one hand, the plant inhibits corrosion due to its antioxidant and antibacterial activities, as stated by [17]. While the research [18] emphasizes that plant-based corrosion inhibitor possesses the complex compound of nitrogen, oxygen, and sulfur atoms of the overall structure that exhibits a similar effect as a synthetic commercial inhibitor.

Great attention to the development of GCI corresponds to their active bioactive molecules. The work [19] proves that the phytochemical content of leaves comprises flavonoids and phenolics that are suitable to inhibit the corrosion process by providing a barrier. However, specifying the mechanical inhibition through the characterization process is critical. A recent report claims that the presence of hydroxyl -OH, ester of -$COOC_2H_5$, carboxylic acids -COOH, and amine functional group -NH_2 are common functional groups in the inhibition process. The *Ammi visnaga* extract was investigated by [20] to evaluate the effect of the phenolic fraction in controlling the corrosion activity of mild steel. The plant extract shows the high efficiencies primarily influence the presence of n-butanol and ethyl acetate in the extract. The publication [21] suggests that the high solubility of ester groups increases the ability of *Novel cationic Gemini ester* surfactant to be considered as GCI. The inhibitor was studied to depress metal dissolution by increasing the hydrophobicity of the inhibitor molecule. In addition, utilizing a highly electronegative atom of oxygen, the role of the corrosion inhibitor containing the amine (-NH_2) group cannot be an oversight.

An updated research finding [22] shows that the mixture of ketone, aldehyde, and amine at their respective proportions maximizes corrosion protection. The inhibitor was used under an oil-gas reservoir and ultra-deep well to modify the damaged surface of the metal effectively. All this suggests that it is advisable to conduct a study on functional group recognition by identification of particular active molecules in plants or chemicals.

In this work, careful attention is given to unveiling the contribution of the functional group of Saga as a corrosion inhibitor. Considering the functional group in Saga, this work shows the development of Saga as GCI as the primary corrosion inhibitor for API 5L Grade B. But there were unaddressed issues related to the contribution of functional groups in determining the adsorption type of inhibitor, particularly of Saga solution. This fundamental impossibility causes inaccuracy in examining whether the monolayer of the passive film [23] is given, or it may approach multiple layers of adsorbed inhibitor. It may be correlated with the reaction mechanism that highlights the inhibitor's oxidation mitigation. Knowing the predicted mechanism unveils the inhibitor's role in forming complex compounds through dative covalent bonding.

Despite the active compound found in the fruit, there were unresolved issues related to its extraction process. The work [24] states that the combination of polar solvents is proven to gain a considerable amount of extract fully. At the same time, the study [25] argues that using autoclaves effectively extracts *Artemisia vulgaris*. The scientist reveals the ether solution through direct soxhlet extraction is sufficient to protect the metal by 93 % while depressing the corrosion rate by nearly 88 %.

The problem statement of this work is correlated with the solvent selection to obtain the primary component of the Saga plant. To our knowledge, the study to unveil the suitability of the solvent corresponds to the composition of alkaloids, saponins, and flavonoid molecules have remained undiscovered. This study is essential to explain the significance of the hydroxyl group and their resonance effect on flavonoid molecules towards the inhibition process in API

5L Grade B under an acidic environment. One way to overcome this difficulty is by selecting a suitable solvent such as methanol that may provide plants' steroids, alkaloids, saponins, and flavonoid molecules. This approach was used to demonstrate that using methanol is ideal to ensure the essential compounds are extracted due to the difference in polarity.

However, it remains unclear how the prepared extract was used to inhibit the corrosion rate on the metal surface. It may be due to the main composition of Saga, such as nitrogen, oxygen, and benzene rings. Also, it has been elaborated that various parts of herbs, such as leaves and fruit, have inherent specific functional groups and electron-rich elements. It is also critical to remember that the molecules comprise heterocyclic atoms and π-electrons, which act as adsorption centers on the metal surface. In common, the high solubility of green inhibitors is correlated with the water solubility and their excellent adsorption through the formation of coordinate bonds [26].

Upon forming a coordinate bond, the adsorption process is related to physisorption, chemisorption, or both. In this setting, the utilization of ΔG_{ads} determines spontaneous adsorption. It is used to predict their reaction feasibility [27], thus making this research practical in correlation with the nature of thermodynamics. All this allows us to assert that it is expedient to conduct a study on developing the natural plant as a green corrosion inhibitor.

3. The aim and objectives of the study

The study aims to offer the potential of Saga as a green corrosion inhibitor under 1M HCl related to its practical utilization in reducing the corrosion rate of carbon steel.

To achieve this aim, the following objectives are accomplished:

– to evaluate the nature of corrosion resistance of API 5L Grade B after dissolution in HCl 1M;

– to identify the primary compounds, which contribute to the inhibitor's adsorption on the surface of CS;

– to analyze the inhibition mechanism corresponding to electrochemical activities using potentiodynamic polarization (PP) and electrochemical impedance spectroscopy (EIS);

– to explain the nature of adsorption by calculating the inhibition's thermodynamic parameters.

4. Materials and methods

4. 1. The object and hypotheses of the study

As previously outlined in Section 3, the chemical content of Saga harnessed the potential of the plant to inhibit the corrosion rate in mild steel. The plant can be found in Indonesia, Sri Lanka, Thailand, South China, India, the Philippines, and South Africa. The primary hypothesis to use Saga as a corrosion inhibitor is due to its elements' main composition, such as nitrogen, oxygen, and benzene rings. Also, it has been elaborated that various parts of herbs, such as leaves and fruit, have inherent specific functional groups and electron-rich elements. It is also critical to remember that the molecules comprise heterocyclic atoms and π-electrons, which act as adsorption centers on the surface of metals. This assumption is justified since the biologically active compound has the conjugation structure to the extent the number of lone pairs of electrons increases the number of adsorption centers; hence it increases the inhibition corrosion effect on mild steel. The appropriate extraction method and how the inhibitory effect is characterized are critical to unveiling the potential of Saga as a corrosion inhibitor.

4. 2. Chemicals and materials

The Abrus precatorius fruits were collected in April 2022 from the local farmer of West Java, Indonesia. The selected extraction process is based on the physicochemical characterization of the fruit to be fully extracted. In the present study, 100 g of plant raw material was mechanically converted to powder and subject to dissolution in 1 dm^3 of methanol for about 24 h. The appearance of sage seed sludge was then filtered using Whatman filter paper no. 42 before drying using a hotplate on the surface of the magnetic stirrer at 40 °C for three hours. The final volume of 700 cm^3 was prepared as the inhibitor solution. The standard solution of HCl 1M was prepared using dilution as previously outlined in [28]. Eventually, the inhibitor solution was obtained as 2, 4, 6, 8, and 10 ml solution.

4. 3. Preparation of the electrode, PP, and EIS measurement

Three-electrode electrochemical measurement was prepared similarly to the publication [29] with a slight modification. The working electrode (WE) was made from API 5L Grade B (10×10×3 mm). The platinum (Pt) electrode and Ag/AgCl electrode served as the counter electrode (CE) and reference electrode (RE). Before conducting the measurement, the WE was polished using 800, 1,000, and 2,000 mesh sandpaper (in turn) and was transferred to a desiccator to ensure the WE was free from air. An open circuit potential (OCP) measurement was conducted on the blank solution (1 M HCl), 2, 4, 6, 8, and 10 ml inhibitor solution using a PGSTAT302 potentiostat. The scanning rate for OCP of PP was set from –1,000 to 1,000 mV with a 500 s scanning rate. The corrosion rate measurement was carried out using ASTM G3 to attain the Tafel extrapolation graph. In this work, the EIS measurement using the scanning range of OCP was –300 to +300 mV using a 1 mV/s scanning rate. The Bode and Nyquist plots were prepared upon the completion of EIS measurement to study the nature of the saga inhibition process.

4. 4. Spectroscopy characterization

The optical emission spectroscopy (OES) and Fourier transform infrared spectroscopy (FTIR) were implemented to provide the elemental composition of substrate and infrared (IR) spectra. The ASTM A751 was used to obtain the maximum percentage composition of CS. The Thermoscientific Nicolet iS-10 FTIR was utilized for the inhibitor analysis to attain the spectroscopic data within the range of 500–4,000 cm^{-1}.

5. Research results of Saga as a green corrosion inhibitor

5. 1. The nature of corrosion resistance of API 5L Grade B after dissolution in HCl 1M

The OES measurement shows the elements' variation in the substrate after the dissolution of API 5L Grade B in HCl 1M, as depicted in Table 1.

Table 1

The OES results

Element	Fe	C	Cr	S	Mn	Mo	Ni	Sn
Composition (%)	98.71	0.205	0.201	0.014	0.481	0.012	0.028	0.054

The substrate is the mild carbon steel shown by the carbon content within 0.05–0.25 %. The study [30] shows the presence of chromium (Cr) at 0.201 % offers the corrosion resistance of steel (Table 1). On the other hand, the high amount of manganese (Mn) of 0.481 % demonstrates that the working electrode remains persistent towards corrosion through grain refinements. Despite the low content of molybdenum (Mo) at 0.012 %, the CS substrate remains substantially corroded.

5. 2. Identification of the primary compounds of inhibitor adsorption in CS results

The FTIR spectra were used to specify the assembly of the saga inhibitor molecules. The results of the FTIR show multiple peaks ranging from 400–4,000 cm^{-1} to provide the actual functional groups or groups of the atom exhibited by the inhibitor (Fig. 1).

The broad peak 3,000–3,500 cm^{1} corresponds to vibration stretch O-H and N-H. While 2,944 cm^{-1} and 2,832 cm^{-1} show $-CH_3$ or $-CH_2$ groups stretch vibration. The weak peak of 1,656–1,800 cm^{-1} relates to the stretching C=O, similar to the publication [31]. The twin peaks at 1499.11 and 1415.18 cm^{-1} correlate to COO vibrations [32]. In addition, the stretch bands of the C-O-C asymmetric stretching of phenol are indicated by the peak of 1114.59 cm^{-1}. It is also important to note that the peak of 1021.93 cm^{-1} corresponds to C-O stretching with C-C vibration [33]. Based on the overall results, the Saga inhibitor is suitable for protecting the metal from corrosion due to the multiple functional groups that can donate electrons to the 3-d atomic orbital.

5. 3. Analysis of the electrochemical inhibition mechanism using EIS and PP results

5. 3. 1. Potentiodynamic polarization results

The Tafel extrapolation behavior of API 5L Grade B in 1M HCl solution shows the effect of *Abrus precatorius* extract as a green corrosion inhibitor, as depicted in Fig. 2.

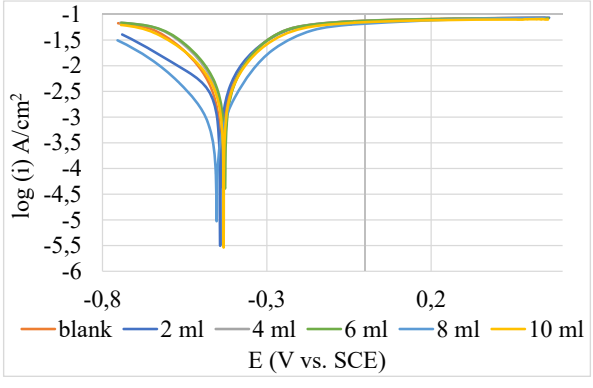

Fig. 2. Tafel plots for various inhibitor concentrations under 1M HCl

Based on Fig. 2, the addition of inhibitor concentration from 2 ml to 10 ml correlates to the shifting of less negative corrosion potential (E_{corr}) despite irregular trends. In addition, it influences the movement of anodic and cathodic branches to lower current corrosion density (i_{corr}). It can be concluded that the AB inhibitor behaves as a semi-mixed-type inhibitor because it influences both corrosion density and the potential of SCE in both regions.

On the contrary, the similar shape of anodic branches demonstrates that the inhibition mechanism is identical for all inhibitor concentrations. The successive addition of inhibitors did not show a significant decrease in corrosion density as in the cathodic region. It also correlated with a sharp decrease in corrosion current density as a result of the evolution of the passive layer, shown in Table 2.

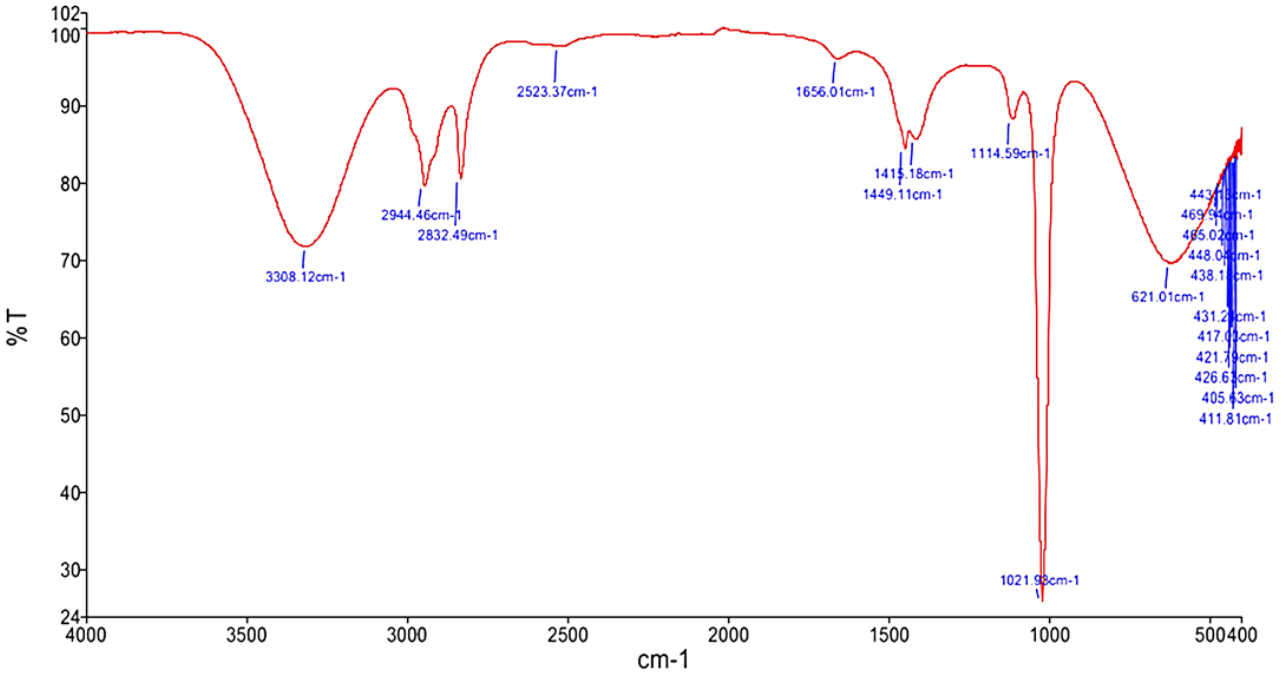

Fig. 1. FTIR results

Table 2

Electrochemical parameters on the potentiodynamic polarization

Conc (ml)	βa (mV)	βc (mV)	Ecorr (mV)	icorr (mA)	Corrosion rate (mmpy)	Inhibition efficiency (%)
Blank	499.12	339.43	−407.16	154.86	1.80	0
2	143.14	264.98	−447.03	33.64	0.39	78 %
4	750.96	783.49	−433.43	28.42	0.33	82 %
6	747.36	649.86	−411.87	26.67	0.31	83 %
8	212.46	252.29	−469.92	24.70	0.29	84 %
10	723.05	561.54	−405.79	21.84	0.25	86 %

Table 2 shows the result of electrochemical parameters, including the Tafel slopes (β_a and β_c), corrosion current density (i_{corr}), corrosion potential (E_{corr}), and their respective corrosion rate and inhibition efficiency. It shows that a higher i_{corr} value of the blank solution is attributed to unprotected mild steel and a high corrosion rate. It can also be reported that the increasing inhibitor concentration lowers the corrosion rate (0.25 mmpy) and increases the inhibition efficiency to 86 %.

In addition to an inhibitor of 2 ml, 4 ml, 6 ml and 8 ml, the corrosion potential values are −447.03 mV, −433.43 mV, −411.87 mV, and −469.92 mV. The corrosion potential shifted in a negative direction, indicating the energy levels of the metal increased. Similar to [25], the change in E_{corr} smaller than 85 mV suggests the change of the reaction mechanism related to the anodic/cathodic dissolving reaction. Eventually, the result in Fig. 2 agrees with the increasing surface coverage area of protection. This indicates that increasing the concentration of AB inhibitor from 2 ml to 10 ml raises the inhibition efficiency from 78 % to 86 %.

5. 3. 2. EIS results

The EIS results diagram comprehends the AB inhibitor's adsorption on the surface of mild steel and is given in the form of a Nyquist plot, Bode plot, and Bode phase (Fig. 3).

The semi-circle diameter of the AB inhibitor increases with the AB concentration to achieve maximum protection of mild steel under acidic conditions (Fig. 3, *a*). This demonstrates the anti-corrosion properties of AB solution before and after the addition of the inhibitor. 10 ml of solution gives the best performance of the inhibitor. In comparison, adding 2 ml of inhibitor is insufficient to protect the metal from corrosive substances shown by the short Nyquist diameter of around 15 Ω cm^2. Likewise, the spectra of 10 ml of inhibitor protect the metal due to the electronic charge transfer process. The difference between the inhibitor's initial and final low-frequency impedance at 10 ml inhibitor solution is 24.3 Ω cm^2. It also correlated with the diameter completion of the capacitive loop as the concentration of inhibitor increases to give optimum impedance value at approximately 33 Ω cm^2.

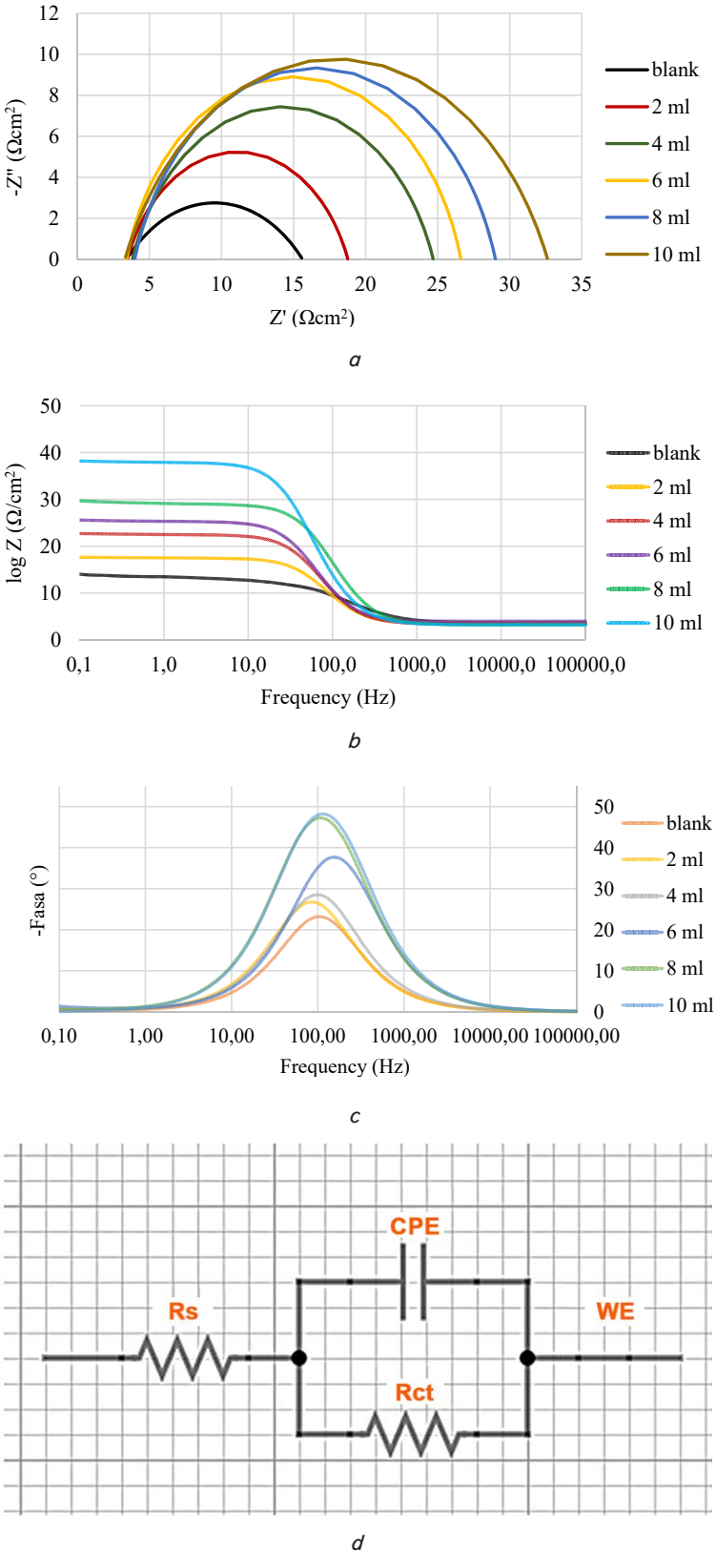

Fig. 3. EIS results of inhibitor: *a* — Nyquist plot; *b* — Bode plot; *c* — Bode phase; *d* — electrical equivalent diagram

The result also agrees with the impact of the Bode plot and Bode phase. The Bode phase shows the frequency range from lower to higher concentration of inhibitor and reached its optimum protection at 27.4 Ω cm^2. This absolute

impedance change agrees with the Nyquist plot's result. At the same time, the solution resistance (R_s), charge transfer resistance (R_{ct}), and capacitance of double-layer (C_{dl}) were enlisted in Table 3. Meanwhile, equation (1) shows the calculation of inhibition efficiency (η) [34].

$$\eta = \left(\frac{i_{corr(0)} - i_{corr(1)}}{i_{corr(0)}} \right) \times 100\% . \quad (1)$$

The charge transfer resistance value of the inhibitor at 10 ml increases almost twice from the blank solution from 12.19 Ω cm^2 to 29.33 Ω cm^2. The result aligns with the depressive value of solution resistance to prove the adsorbed inhibitor evolution on the surface of mild steel (Table 3).

Table 3

Electrical elements on EIS methods with the variation of concentration

Conc (ml)	R_s (Ω·cm^2)	R_{ct} (Ω·cm^2)	C_{dl} (μF·cm^2)	n	Inhibition efficiency (%)
Blank	4.42	12.19	2411.00	0.54	–
2	10.06	15.31	689.65	0.76	34.06
4	9.81	20.88	511.66	0.79	51.64
6	3.41	23.20	460.45	0.83	56.48
8	12.98	25.03	459.00	0.82	59.67
10	7.30	29.33	420.16	0.75	65.58

On the other hand, the rapid decrease of C_{dl} is associated with the increased value of R_{ct} and their ability to replace more water molecules. Linearly, the inhibition efficiency increases by nearly 66 % at 10 ml inhibitor solution (Table 3). The difference in inhibition efficiency between the polarization curve and EIS measurement is 20 % indicating a slight correlation between them due to the apparent response toward thickness evolution of the passive layer [35]. Studying the surface inhomogeneity of the mild steel surface related to the adsorption process is critical. It is possible to deduce that the value of n or CPE shows the surface inhomogeneity after adding an inhibitor. The increase of n of nearly 0.8 proves the inhibitor's adsorption has increased the surface smoothness and reduced the number of corrosion pits. The result of EIS fits the electrical equivalent diagram as illustrated in Fig. 3, *d*.

The above result suggests the mechanistic inhibition based on Table 3 and Fig. 3. Hence, the inhibition mechanism is proposed and provided in equation (3), as previously outlined in [36].

$$\left\{ \begin{array}{l} Fe + Cl^- \rightarrow \left(FeCl^-\right)_{ads} \\ \left(FeCl^-\right)_{ads} \rightarrow \left(FeCl\right)_{ads} + e^- \\ \left(FeCl\right)_{ads} \rightarrow FeCl^+ + e^- \\ FeCl^+ \rightarrow Fe^{2+} + Cl^- \\ Fe^{2+} + Cl^- + Inh \rightarrow \left[Fe^{2+} - Cl - Inh\right]^+_{ads} \end{array} \right\}. \quad (3)$$

The chloride ions attack the iron atom while it releases the electron and forms $FeCl^+$. However, under highly corrosive substances, it dismisses Fe^{2+} and Cl^-. The higher inhibitor concentration is bound with the ions to give the positive complex adsorption layer. The evolution of the thickness layer corresponds to a higher value of R_{ct} for the whole inhibitor concentrations, which lowers the capacitance double layer value (C_{dl}).

5. 4. Thermodynamic parameters from the adsorption isotherm calculation results

The feasibility of adsorbed inhibitors on the surface of the metal depends on the thermodynamic parameters. The assigned ΔG_{ads}, ΔS_{ads}, and ΔH_{ads} show the nature of inhibition and determine whether the strength of the adsorption process increases as the function of surface coverage area. Table 4 depicts the results of the thermodynamic calculation to show the effect of concentration in increasing the surface area of protection.

Table 4

Surface coverage (θ) with the variation of inhibitor concentration

Conc (mol/L)	θ	K_{ads}	ΔG_{ads} (kJ/mol)
2	0.78	0.4164	–35.26
4	0.82	0.7265	–36.03
6	0.83	0.8319	–36.29
8	0.84	0.9081	–36.47
10	0.86	1.0665	–36.87

It can be reported that as the concentration of inhibitor increases, the surface coverage area increases (Table 4). This is attributed to the increased value of $R_{ct,}$ which thickens the barrier between the substrate and the acidic solution; thus, it reaches maximum protection of 0.86. This setting requires 10 ml of AB inhibitor to protect 1 cm^2 of substrate surface area, giving 65.56 % inhibition efficiency. Furthermore, the experimental data related to various isothermic adsorption are presented in Fig. 4.

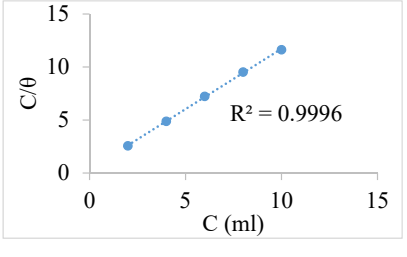

a

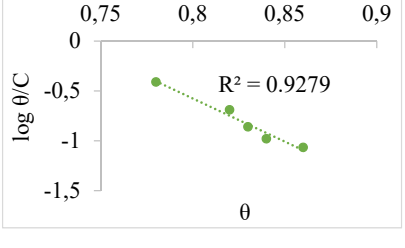

b

Fig. 4. Adsorption isotherm: *a* — Langmuir; *b* — Temkin

Based on the plotting, the nearness of the R^2 value to 1 claims the Langmuir adsorption isotherm model instead of Temkin. The linearity between the formation of the mono-

layer passive film and the substrate prevents the number of corrosion sites due to high dissolution under acidic conditions.

Equation (2) shows the calculation of the adsorption/desorption equilibrium constant of K_{ads} (mol·L^{-1}).

$$\frac{C}{\theta}=\frac{1}{K_{ads}}+C. \quad (2)$$

In the above equation, C is the inhibitor concentration (mol dm^{-3}) and θ is the surface coverage area. According to Table 4, the adsorption type of Saga inhibitor is the chemisorption ΔG_{ads} −36.87 kJ/mol. Due to the low value of ΔG_{ads}, the chemical interaction confirms the value of R^2, in which the evolution of passive film forms monolayer adsorption [37]. Also, the magnitude of ΔG_{ads} demonstrates the feasibility of the inhibitor, and the high value of K_{ads} shows their stability in the 10 ml inhibitor solution.

6. Discussion of Saga as a green corrosion inhibitor

In this work, the working electrode was severely corroded owing to dissolution in HCl 1M. Therefore, it is necessary to learn the composition of metal damage structure and allow the change of chemical composition in API 5 L Grade B. The research [38] shows the Cr, Mn, and Mo content is 0.069 %, 0.888 %, and 0.039 %, respectively. This composition typifies the actual specification of API 5L Grade B. Based on Table 1, the working electrode of API 5L Grade B bears the carbon content of 0.205, which specifies the mild carbon steel of ASTM A53. The work [39] shows that the metal has low corrosion resistance, requiring intensive protection to reduce the effect of corrosion.

In this work, the Saga inhibitor acts as a barrier to inhibit the possible dissolution of metal due to the adsorption process. As stated in Section 5, the chromium content of 0.201 % is inadequate to improve the corrosion resistance of the working electrode despite the continuous and dense formation of Cr-rich film (Cr_2O_3) [40]. The film is accountable for reducing the corrosion effect by forming an overlapping 3d orbital of Cr with the 2p orbital of O. However, the low content of Cr (Table 1) requires intensive adsorption of an inhibitor to repair the dissolution of metal.

In addition, the presence of manganese (Mn) generally contributes to the coating resistance to corrosion, as stated by the previous publication [41]. Our study shows lower Mn content at 0.481 %, which induces metal susceptibility to corrosion in the long run. Hence, it can be concluded that adding 10 ml of Saga inhibitor is sufficient to control the corrosion rate at 0.25 mmpy as provided in Table 2. In this setting, the dramatic corrosion rate can be associated with the adsorption of corrosion inhibitor of metals.

On the other hand, the low composition of Mo shown in the working electrode may have further oxidized to MoO_3 and lowered the protection of the metal. In this process, the oxidation of Mo_2O_5 to give MoO_3 indicates the dismissal of electrons and causes metal corrosion.

The FTIR characterization is used to gain deeper insight into the chemical structure of the Saga inhibitor. Based on the results of FTIR, the Saga inhibitor comprises several active molecules such as C=O, C=C, C-O, and O-H, which become a center of inhibitor adsorption [42]. The extra lone pair of electrons on oxygen atoms increases the formation of a dative covalent bond.

Based on Fig. 2, the peak at 3308 cm^{-1} indicates O-H stretching vibrations of alcohol. In contrast, the phenol compounds are shown at 3200–3600 cm^{-1}. The results are comparable to the work [43], which offers a similar absorption peak. Furthermore, the appearance peak at nearly 3200 cm^{-1} correlates with the formation of the Fe-OH complex and indicates the inhibition process has occurred [44]. Therefore, this confirms that the hydroxyl groups participate in the adsorption process to form the passive film.

The height at 2,944 cm^{-1} and 2,832 cm^{-1} indicates C-H stretching vibrations are related to methylene groups CH_2 alkane compounds [45]. The peak at 1,656 cm^{-1} suggests C=O stretching vibrations, based on the wavenumbers correlation 1,650–1,800 cm^{-1}. The work [46] reports that the carbonyl functional groups are responsible for developing a dative covalent bond with the metal surface and increasing the shielding film evolution on the carbon steel.

Moreover, the peak at 1,499 cm^{-1} and 1415.18 cm^{-1} indicates C=C stretching vibrations of aromatic compounds. The peak at 1,114 cm^{-1} and 1,021 cm^{-1} demonstrates the C-O stretching vibrations of alcohol and phenol compounds. One of the adsorption parameters is the inhibition efficiency, which correlated to the appearance of the highly electronegative heteroatoms and π-conjugation and the electron donating substituent groups [47]. The presence of C=C and C-O facilitates the above requirement as it would actively strengthen the adsorption/desorption bonding strength. This result agrees with the high value of K_{ads}, as stated in Table 4.

On the other hand, the potentiodynamic polarization curves at various concentrations show the inhibition mechanism of the Saga inhibitor. In this characterization process, the concentration of 10 ml inhibitor shows the best inhibitor compared to the blank sample solution. The reduction of one order of magnitude from corrosion current density between the high concentration solution (10 ml) and the blank solution confirms the excellent role of the active functional group. This adsorption capability primarily interrupts the anodic and cathodic sites [48]. However, the cathodic region dominates the inhibition process (Fig. 2). The cathodic behavior confirms that the inhibitor actively inhibits the dissolution process by dismissing electrons from the metal and depresses E_{corr} at −405.79 mV. Simultaneously, the same effect influences the rapid increase of the cathodic Tafel slope from 252.20 mV to 561.54 mV and increases the inhibition efficiency at 86 %.

Furthermore, the inhibition characteristic of the Saga inhibitor to protect steel from HCl 1M was evaluated using EIS. According to Fig. 3, *a*, the one-relaxation time and the depression shape of the arc in the Nyquist plot show no observable changes. The inhibition mechanism did not alter despite adding inhibitors at various concentrations. Moreover, the interface reaction between the inhibitor solution and metal dominates due to the charge transfer process [49]. This result indicates the formation of coordinate bonding and complex substance in several functional groups shown in the FTIR results.

On the other hand, the outcomes of the Bode plot confirm the Bode phase angle. In Fig. 3, *b*, the two-time constants of the Bode phase are related to the dielectric properties of the inhibitor, which acts as a charged capacitor to restrict the electrochemical reaction. Meanwhile, the 10 ml solution shows the presence of two smaller shoulders. It offers the maximum inhibitor protection and passivation of

inhibitor (Fig. 3, *b*). Moreover, the magnitude of impedance modulation rises when a higher concentration is added at a lower frequency, showing the passive film protects the steel surface from corrosion. In addition, the steady increment of phase angle at −1.77° [50] indicates the increasing capacitive on the smoother metal surface through rapid reduction from corrosive substance. The phenomenon confirms the result of the Nyquist plot, where the inhomogeneity and roughness of corroding metal are reduced to displace more water and chloride ions with the inhibitor molecules [51]. As stated in the previous section, the contribution of n at 10 ml of inhibitor confirms the finding given from the Nyquist plot. At the same concentration, the high value of n demonstrates the growth of a single layer inhibitor to protect the metal from HCl solution fully.

Increasing corrosion protection shows a piece of evidence on how the Saga inhibitor protects the metal, as provided in Fig. 3, *d*. The use of Saga solution in a lower pH environment offers resistance from the adsorbed film on the surface of the substrate while increasing the value of the inhibitor solution of R_{ct}. Therefore, the one-time equivalent circuit can be proposed to fit the experimental values of EIS data (Fig. 3, *d*) [52]. In this setting, the fitting parameters of charge transfer resistance of R_{ct}, solution resistance of $R_{s,}$ and constant phase element from the double layer of CPE inhibitor were collected. The information gives insight into earning the mechanistic inhibition (Table 3, Fig. 3). Hence, the inhibition mechanism is proposed and provided in equation (3), as previously outlined in [36].

The inhibition correlates to the types of adsorption classification either through physisorption or chemisorption. Based on Table 4, the value of ΔG_{ads} is −36.87 kJ/mol. It corresponds to the formation of the dative-covalent bond between the adsorbate and the mild steel through electron donation (chemisorption). The research [53] argues that the strength of their bonding commonly measures the adsorption process. In this scenario, the low value of ΔG_{ads} suggests that the adsorption process occurs spontaneously with an indication of the monolayer of inhibitor film. The same result confirms the mixed-type behavior and abides by Langmuir isotherm adsorption of most plant extracts, which is similar to the existing report [54]. The fact aligns with the development of Langmuir isotherm adsorption, where the nearness of R^2 is 1.

Despite the above description in terms of Saga as a corrosion inhibitor, careful attention to the impact of surface treatment should not be undermined. The limitation of this study includes the examination related to the composition and the surface condition of the metal. The surface characterization as the effect of corroding material provides valuable information on how the inhibitor protects the steel. It correlates to the observation of a sharp reduction in pitting corrosion sites and the elemental identification on the metal surface. Scanning electron microscopy (SEM) aided by energy dispersive X-ray analysis (EDX) is suitable to meet the above limitation. Furthermore, a possible step of using high SEM on the cross-section region and reconsidering using cyclic potentiodynamic polarization would be favorable to optimize the actual concentration inhibitor in reducing the effect of corrosion.

In more detail, the above characterization process showcases valuable information on various comparisons between the corroded and un-corroded surfaces. It is expected that the aggressive attack of HCl 1M solution causes the damaged surface of steel and several inherent imperfections. On the contrary, the adsorption of inhibitors modifies the surface morphology by reducing the roughness of the damaged surface. This process speeds up through the gradual evolution of passive film as the concentration of inhibitor increases.

Utilizing atomic force spectroscopy (AFM) is expected to confirm the surface inhomogeneity post addition of inhibitor. The primary aim of using AFM is to confirm the result of SEM, where the addition of an inhibitor decreases the number of pit depths of the damaged surface due to quickening adsorption of the inhibitor. The surface roughness of the mild steel is indicated by the value of the skewness parameter, where its low value indicates the feasibility of the adsorption process. The result also explains the applicability of using the surface contact test to determine the increased hydrophobicity of metal surfaces upon the addition of inhibitors. It affects more water molecules being repelled to mitigate metals dissolution when exposed to HCl 1M solution. As a result, the more hydrophobic the surface, the higher the contact angle to prove the perfect protection of inhibitor post addition.

Another study restriction was low inhibition efficiency when the Saga inhibitor was characterized using EIS. It is assumed that mixing the inhibitor with the intensifier of some ionic liquid would enhance the number of donated electrons to the 3d orbital of metals. Utilizing the ionic liquid is considered the development of successive research since it would repair the thermal stability of inhibitors at elevated temperatures. The intensifier's role is to increase the number of electron donation sites, hence the higher possibility of establishing chemical bonding between the inhibitor and the substrate. As a result, the synergistic effect between the inhibitor and the ionic liquid causes a more significant effect to increase the bond strength, including the greater surface area of protection from the corrosive solution of HCl 1M.

Notably, the present work has not elaborated on the specific contribution of temperature variation beyond 298 K, or it tends to disadvantage the study. An alternative solution to address the challenge is varying the range temperature between 303–323 K. The thermodynamic results, including the determination of activation energy, are considered suitable to earn the actual types of adsorption to gain a deeper insight into the inhibition performance of the inhibitor. In addition, the subsequent potent research may correlate with the substrate's vertical side and determine the potential passivation value. The passivation is expected to correlate to the protected metal's anticorrosive surface. At the same time, the higher anti-corrosion passive layer results from the even distributed adsorption of the inhibitor.

7. Conclusions

1. API 5L Grade B corrosion resistance has gradually decreased upon metal immersion into HCl 1M. The change of composition in chromium, manganese, and molybdenum reduces metal protection from corrosive substances and requires immediate protection from the Saga inhibitor. At higher concentrations, the inhibitor lowers the corrosion current density at 21.84 mmpy through the development of passive film and inhibits the rate of electron dismissal from the 3d atom of metals.

2. In the present study, the main compounds of the inhibitor comprise C=O, C=C, C-O-C, and benzene as the primary contributor to the adsorption. The FTIR results show the

intensive variation of multiple functional groups behaves as a donor electron or electron donating group. As a result, it quickens the inhibition process and demonstrates many active components to participate in the passive film evolution thickness.

3. According to EIS and PP results, the increase of inhibitor resistance correlated with the increasing Nyquist plot's diameter, more negative Bode phase angle, and the broader shoulder in the Bode plot. At the same time, it lowers the capacitance of the double layer and increases the dielectric capacitance. As a result, the inhibition efficiency stays at 86 % (PP) and 65.58 % (EIS) to broaden the surface coverage area of protection.

4. According to the results of the thermodynamic calculation, the interaction between the inhibitor and substrate occurs chemically. The negative value of ΔG_{ads} shows the feasibility of the inhibitor to adsorb at the surface of the metal and continue to increase at higher concentrations.

Conflict of interest

The authors declare that they have no conflict of interest in relation to this research, whether financial, personal, authorship or otherwise, that could affect the research and its results presented in this paper.

Acknowledgments

All the authors contributed equally to the manuscript. The authors declare no known conflict, financial interests, or personal relationships that could have affected the work reported in this paper. The author gratefully thanks the Ministry of Research and Technology/National Research and Innovation Agency for the financial support of contract number NKB-857/UN2.RST/HKP.05.00/2022.

References

1. Ekere, I., Agboola, O., Eshorane Sanni, S. (2019). DNA from Plant leaf Extracts: A Review for Emerging and Promising Novel Green Corrosion Inhibitors. Journal of Physics: Conference Series, 1378, 022049. doi: https://doi.org/10.1088/1742-6596/1378/2/022049
2. Alaneme, K. K., Olusegun, S. J., Alo, A. W. (2016). Corrosion inhibitory properties of elephant grass (Pennisetum purpureum) extract: Effect on mild steel corrosion in 1M HCl solution. Alexandria Engineering Journal, 55 (2), 1069–1076. doi: https://doi.org/10.1016/j.aej.2016.03.012
3. Aditiyawarman, T., Kaban, A. P. S., Soedarsono, J. W. (2022). A Recent Review of Risk-Based Inspection Development to Support Service Excellence in the Oil and Gas Industry: An Artificial Intelligence Perspective. ASCE-ASME J Risk and Uncert in Engrg Sys Part B Mech Engrg, 9 (1). doi: https://doi.org/10.1115/1.4054558
4. Prifiharni, S., Mashanafie, G., Priyotomo, G., Royani, A., Ridhova, A., Elya, B., Soedarsono, J. W. (2022). Extract sarampa wood (Xylocarpus Moluccensis) as an eco-friendly corrosion inhibitor for mild steel in HCl 1M. Journal of the Indian Chemical Society, 99 (7), 100520. doi: https://doi.org/10.1016/j.jics.2022.100520
5. Pramana, R. I., Kusumastuti, R., Soedarsono, J. W., Rustandi, A. (2013). Corrosion Inhibition of Low Carbon Steel by Pluchea Indica Less. in 3.5% NaCL Solution. Advanced Materials Research, 785-786, 20–24. doi: https://doi.org/10.4028/www.scientific.net/amr.785-786.20
6. Subekti, N., Soedarsono, J. W., Riastuti, R., Sianipar, F. D. (2020). Development of environmental friendly corrosion inhibitor from the extract of areca flower for mild steel in acidic media. Eastern-European Journal of Enterprise Technologies, 2 (6 (104)), 34–45. doi: https://doi.org/10.15587/1729-4061.2020.197875
7. Kusumastuti, R., Pramana, R. I., Soedarsono, J. W. (2017). The use of morinda citrifolia as a green corrosion inhibitor for low carbon steel in 3.5% NaCl solution. AIP Conference Proceedings. doi: https://doi.org/10.1063/1.4978085
8. Kaban, E. E., Maksum, A., Permana, S., Soedarsono, J. W. (2018). Utilization of secang heartwood (caesalpinia sappan l) as a green corrosion inhibitor on carbon steel (API 5L Gr. B) in 3.5% NaCl environment. IOP Conference Series: Earth and Environmental Science, 105, 012062. doi: https://doi.org/10.1088/1755-1315/105/1/012062
9. Azmi, M. F., Soedarsono, J. W. (2018). Study of corrosion resistrance of pipeline API 5L X42 using green inhibitor bawang dayak (Eleutherine americanna Merr.) in 1M HCl. IOP Conference Series: Earth and Environmental Science, 105, 012061. doi: https://doi.org/10.1088/1755-1315/105/1/012061
10. Kaban, A. P. S., Ridhova, A., Priyotomo, G., Elya, B., Maksum, A., Sadeli, Y. et. al. (2021). Development of white tea extract as green corrosion inhibitor in mild steel under 1 M hydrochloric acid solution. Eastern-European Journal of Enterprise Technologies, 2 (6 (110)), 6–20. doi: https://doi.org/10.15587/1729-4061.2021.224435
11. Paul Setiawan Kaban, A., Mayangsari, W., Syaiful Anwar, M., Maksum, A., Riastuti, R., Aditiyawarman, T., Wahyuadi Soedarsono, J. (2022). Experimental and modelling waste rice husk ash as a novel green corrosion inhibitor under acidic environment. Materials Today: Proceedings, 62, 4225–4234. doi: https://doi.org/10.1016/j.matpr.2022.04.738
12. Rajalakshmi, R., Subhashini, S., Nanthini, M., Srimathi, M. (2009). Inhibiting effect of seed extract of Abrus precatorius on corrosion of aluminium in sodium hydroxide. Oriental Journal of Chemistry, 25 (2). URL: http://www.orientjchem.org/vol25no2/inhibiting-effect-of-seed-extract-of-abrus-precatorius-on-corrosion-of-aluminium-in-sodium-hydroxide-2/
13. Aribo, S., Olusegun, S. J., Ibhadiyi, L. J., Oyetunji, A., Folorunso, D. O. (2017). Green inhibitors for corrosion protection in acidizing oilfield environment. Journal of the Association of Arab Universities for Basic and Applied Sciences, 24 (1), 34–38. doi: https://doi.org/10.1016/j.jaubas.2016.08.001

14. Dehghani, A., Bahlakeh, G., Ramezanzadeh, B. (2019). A detailed electrochemical/theoretical exploration of the aqueous Chinese gooseberry fruit shell extract as a green and cheap corrosion inhibitor for mild steel in acidic solution. Journal of Molecular Liquids, 282, 366–384. doi: https://doi.org/10.1016/j.molliq.2019.03.011
15. Rustandi, A., Soedarsono, J. W., Suharno, B. (2011). The Use of Mixture of Piper Betle and Green Tea as a Green Corrosion Inhibitor for API X-52 Steel in Aerated 3.5 % NaCl Solution at Various Rotation Rates. Advanced Materials Research, 383-390, 5418–5425. doi: https://doi.org/10.4028/www.scientific.net/amr.383-390.5418
16. Singh, W. P., Bockris, J. O. M. (1996). Toxicity issues of organic corrosion inhibitors: Applications of QSAR model. Conference: National Association of Corrosion Engineers (NACE) annual corrosion conference and exposition: water and waste water industries. Denver. URL: https://www.osti.gov/biblio/397824-toxicity-issues-organic-corrosion-inhibitors-applications-qsar-model
17. Berrissoul, A., Ouarhach, A., Benhiba, F., Romane, A., Zarrouk, A., Guenbour, A. et. al. (2020). Evaluation of Lavandula mairei extract as green inhibitor for mild steel corrosion in 1 M HCl solution. Experimental and theoretical approach. Journal of Molecular Liquids, 313, 113493. doi: https://doi.org/10.1016/j.molliq.2020.113493
18. Cherrad, S. et. al. (2015). Unveiling corrosion inhibition properties of the Cupressus Arizonica leaves essential oil for carbon steel in 1.0 M HCl. International Journal of Corrosion and Scale Inhibition. doi: https://doi.org/10.17675/2305-6894-2020-9-2-15
19. Schreiner, M., Huyskens-Keil, S. (2006). Phytochemicals in Fruit and Vegetables: Health Promotion and Postharvest Elicitors. Critical Reviews in Plant Sciences, 25(3), 267–278. doi: https://doi.org/10.1080/07352680600671661
20. Aourabi, S., Driouch, M., Sfaira, M., Mahjoubi, F., Hammouti, B., Verma, C. et. al. (2021). Phenolic fraction of Ammi visnaga extract as environmentally friendly antioxidant and corrosion inhibitor for mild steel in acidic medium. Journal of Molecular Liquids, 323, 114950. doi: https://doi.org/10.1016/j.molliq.2020.114950
21. Mao, T., Huang, H., Liu, D., Shang, X., Wang, W., Wang, L. (2021). Novel cationic Gemini ester surfactant as an efficient and eco-friendly corrosion inhibitor for carbon steel in HCl solution. Journal of Molecular Liquids, 339, 117174. doi: https://doi.org/10.1016/j.molliq.2021.117174
22. Jiang, J. et. al. (2020). Optimization of Preparation Method for Ketoaldehyde Amine Condensate High Temperature Corrosion Inhibitor. Oilf. Chem., 37 (02). doi: https://doi.org/10.19346/j.cnki.1000-4092.2020.02.025
23. Cornette, P., Costa, D., Marcus, P. (2017). DFT Modelling of Cu Segregation in Al-Cu Alloys Covered by an Ultrathin Oxide Film and Possible Links with Passivity. Metals, 7 (9), 366. doi: https://doi.org/10.3390/met7090366
24. Abedini, A., Amiri, H., Karimi, K. (2020). Efficient biobutanol production from potato peel wastes by separate and simultaneous inhibitors removal and pretreatment. Renewable Energy, 160, 269–277. doi: https://doi.org/10.1016/j.renene.2020.06.112
25. Pineda Hernández, D. A., Restrepo Parra, E., Arango Arango, P. J., Segura Giraldo, B., Acosta Medina, C. D. (2021). Innovative Method for Coating of Natural Corrosion Inhibitor Based on Artemisia vulgaris. Materials, 14 (9), 2234. doi: https://doi.org/10.3390/ma14092234
26. Guo, L., Obot, I. B., Zheng, X., Shen, X., Qiang, Y., Kaya, S., Kaya, C. (2017). Theoretical insight into an empirical rule about organic corrosion inhibitors containing nitrogen, oxygen, and sulfur atoms. Applied Surface Science, 406, 301–306. doi: https://doi.org/10.1016/j.apsusc.2017.02.134
27. Berdimurodov, E., Kholikov, A., Akbarov, K., Guo, L., Kaya, S., Katin, K. P. et. al. (2022). Novel gossypol–indole modification as a green corrosion inhibitor for low–carbon steel in aggressive alkaline–saline solution. Colloids and Surfaces A: Physicochemical and Engineering Aspects, 637, 128207. doi: https://doi.org/10.1016/j.colsurfa.2021.128207
28. Bhatia, M., Siddiqui, N. A., Gupta, S. (2013). Abrus Precatorius (L.): An Evaluation of Traditional Herb. Indo American Journal of Pharmaceutical Research, 3 (4). URL: https://lavierebelle.org/IMG/pdf/abrus_precatorius_an_evaluation_of_a_traditional_plant.pdf
29. Baran, E., Cakir, A., Yazici, B. (2019). Inhibitory effect of Gentiana olivieri extracts on the corrosion of mild steel in 0.5 M HCl: Electrochemical and phytochemical evaluation. Arabian Journal of Chemistry, 12 (8), 4303–4319. doi: https://doi.org/10.1016/j.arabjc.2016.06.008
30. Joseph, B., John, S., Joseph, A., Narayana, B. (2010). Imidazolidine-2-thione as corrosion inhibitor for mild steel in hydrochloric acid. Indian J. Chem. Technol., 17, 366–374. URL: http://nopr.niscpr.res.in/bitstream/123456789/10452/1/IJCT%2017%285%29%20366-374.pdf
31. Poojary, N. G., Kumari, P., Rao, S. A. (2021). 4-Hydroxyl-N′-[(3-Hydroxy-4-Methoxyphenyl) Methylidene] Benzohydrazide] as Corrosion Inhibitor for Carbon Steel in Dilute H2SO4. Journal of Failure Analysis and Prevention, 21, 1264–1273. doi: https://doi.org/10.1007/s11668-021-01166-y
32. El Azzouzi, M., Azzaoui, K., Warad, I., Hammouti, B., Shityakov, S., Sabbahi, R. et. al. (2022). Moroccan, Mauritania, and senegalese gum Arabic variants as green corrosion inhibitors for mild steel in HCl: Weight loss, electrochemical, AFM and XPS studies. Journal of Molecular Liquids, 347, 118354. doi: https://doi.org/10.1016/j.molliq.2021.118354
33. Palimi, M. J., Tang, Y., Alvarez, V., Kuru, E., Li, D. Y. (2022). Green corrosion inhibitors for drilling operation: New derivatives of fatty acid-based inhibitors in drilling fluids for 1018 carbon steel in CO2-saturated KCl environments. Materials Chemistry and Physics, 288, 126406. doi: https://doi.org/10.1016/j.matchemphys.2022.126406
34. Berrissoul, A., Ouarhach, A., Benhiba, F., Romane, A., Guenbour, A., Outada, H. et. al. (2022). Exploitation of a new green inhibitor against mild steel corrosion in HCl: Experimental, DFT and MD simulation approach. Journal of Molecular Liquids, 349, 118102. doi: https://doi.org/10.1016/j.molliq.2021.118102

35. Sharma, S., Ganjoo, R., Kr. Saha, S., Kang, N., Thakur, A., Assad, H. et. al. (2021). Experimental and theoretical analysis of baclofen as a potential corrosion inhibitor for mild steel surface in HCl medium. Journal of Adhesion Science and Technology, 1–26. doi: https://doi.org/10.1080/01694243.2021.2000230
36. Dahiya, S., Kumar, P., Lata, S., Kumar, R., Dahiya, N., Ahlawat, S. (2017). An exhaustive study of a coupling reagent (1-(3-dimethylaminopropyl) 3-ethylcarbodiimide hydrochloride) as corrosion inhibitor for steel. Indian Journal of Chemical Technology, 24 (3), 327–335. URL: https://www.researchgate.net/publication/317175437_An_exhaustive_study_of_a_coupling_reagent_1-3-dimethylaminopropyl_3-ethylcarbodiimide_hydrochloride_as_corrosion_inhibitor_for_steel
37. Parveen, G., Bashir, S., Thakur, A., Saha, S. K., Banerjee, P., Kumar, A. (2019). Experimental and computational studies of imidazolium based ionic liquid 1-methyl- 3-propylimidazolium iodide on mild steel corrosion in acidic solution. Materials Research Express, 7 (1), 016510. doi: https://doi.org/10.1088/2053-1591/ab5c6a
38. Velázquez, J. C., González-Arévalo, N. E., Díaz-Cruz, M., Cervantes-Tobón, A., Herrera-Hernández, H., Hernández-Sánchez, E. (2022). Failure pressure estimation for an aged and corroded oil and gas pipeline: A finite element study. Journal of Natural Gas Science and Engineering, 101, 104532. doi: https://doi.org/10.1016/j.jngse.2022.104532
39. Lgaz, H., Chung, I.-M., Albayati, M. R., Chaouiki, A., Salghi, R., Mohamed, S. K. (2020). Improved corrosion resistance of mild steel in acidic solution by hydrazone derivatives: An experimental and computational study. Arabian Journal of Chemistry, 13 (1), 2934–2954. doi: https://doi.org/10.1016/j.arabjc.2018.08.004
40. Gu, Y., Xu, Y., Shi, Y., Feng, C., Volodymyr, K. (2022). Corrosion resistance of 316 stainless steel in a simulated pressurized water reactor improved by laser cladding with chromium. Surface and Coatings Technology, 441, 128534. doi: https://doi.org/10.1016/j.surfcoat.2022.128534
41. Khast, F., Saybani, M., Sarabi Dariani, A. A. (2022). Effects of copper and manganese cations on cerium-based conversion coating on galvanized steel: Corrosion resistance and microstructure characterizations. Journal of Rare Earths, 40 (6), 1002–1006. doi: https://doi.org/10.1016/j.jre.2021.07.015
42. Sharma, S., Ganjoo, R., Kr. Saha, S., Kang, N., Thakur, A., Assad, H., Kumar, A. (2022). Investigation of inhibitive performance of Betahistine dihydrochloride on mild steel in 1 M HCl solution. Journal of Molecular Liquids, 347, 118383. doi: https://doi.org/10.1016/j.molliq.2021.118383
43. Elemike, E. E., Nwankwo, H. U., Onwudiwe, D. C. (2019). Synthesis and comparative study on the anti-corrosion potentials of some Schiff base compounds bearing similar backbone. Journal of Molecular Liquids, 276, 233–242. doi: https://doi.org/10.1016/j.molliq.2018.11.161
44. Li, X.-H., Deng, S.-D., Fu, H. (2010). Inhibition by Jasminum nudiflorum Lindl. leaves extract of the corrosion of cold rolled steel in hydrochloric acid solution. Journal of Applied Electrochemistry, 40 (9), 1641–1649. doi: https://doi.org/10.1007/s10800-010-0151-5
45. Shahmoradi, A. R., Ranjbarghanei, M., Javidparvar, A. A., Guo, L., Berdimurodov, E., Ramezanzadeh, B. (2021). Theoretical and surface/electrochemical investigations of walnut fruit green husk extract as effective inhibitor for mild-steel corrosion in 1M HCl electrolyte. Journal of Molecular Liquids, 338, 116550. doi: https://doi.org/10.1016/j.molliq.2021.116550
46. Salmasifar, A., Edraki, M., Alibakhshi, E., Ramezanzadeh, B., Bahlakeh, G. (2021). Combined electrochemical/surface investigations and computer modeling of the aquatic Artichoke extract molecules corrosion inhibition properties on the mild steel surface immersed in the acidic medium. Journal of Molecular Liquids, 327, 114856. doi: https://doi.org/10.1016/j.molliq.2020.114856
47. Chauhan, D. S., Verma, C., Quraishi, M. A. (2021). Molecular structural aspects of organic corrosion inhibitors: Experimental and computational insights. Journal of Molecular Structure, 1227, 129374. doi: https://doi.org/10.1016/j.molstruc.2020.129374
48. Ma, I. A. W., Ammar, S., Kumar, S. S. A., Ramesh, K., Ramesh, S. (2021). A concise review on corrosion inhibitors: types, mechanisms and electrochemical evaluation studies. Journal of Coatings Technology and Research, 19 (1), 241–268. doi: https://doi.org/10.1007/s11998-021-00547-0
49. Khamseh, S., Alibakhshi, E., Ramezanzadeh, B., Sari, M. G., Nezhad, A. K. (2020). Developing a Graphite like Carbon:Niobium thin film on GTD-450 stainless steel substrate. Applied Surface Science, 511, 145613. doi: https://doi.org/10.1016/j.apsusc.2020.145613
50. Haque, J., Verma, C., Srivastava, V., Nik, W. B. W. (2021). Corrosion inhibition of mild steel in 1M HCl using environmentally benign Thevetia peruviana flower extracts. Sustainable Chemistry and Pharmacy, 19, 100354. doi: https://doi.org/10.1016/j.scp.2020.100354
51. Hamani, H., Douadi, T., Al-Noaimi, M., Issaadi, S., Daoud, D., Chafaa, S. (2014). Electrochemical and quantum chemical studies of some azomethine compounds as corrosion inhibitors for mild steel in 1M hydrochloric acid. Corrosion Science, 88, 234–245. doi: https://doi.org/10.1016/j.corsci.2014.07.044
52. Asadi, N., Ramezanzadeh, M., Bahlakeh, G., Ramezanzadeh, B. (2019). Utilizing Lemon Balm extract as an effective green corrosion inhibitor for mild steel in 1M HCl solution: A detailed experimental, molecular dynamics, Monte Carlo and quantum mechanics study. Journal of the Taiwan Institute of Chemical Engineers, 95, 252–272. doi: https://doi.org/10.1016/j.jtice.2018.07.011
53. Sims, R., Harmer, S., Quinton, J. (2019). The Role of Physisorption and Chemisorption in the Oscillatory Adsorption of Organosilanes on Aluminium Oxide. Polymers, 11 (3), 410. doi: https://doi.org/10.3390/polym11030410
54. Alrefaee, S. H., Rhee, K. Y., Verma, C., Quraishi, M. A., Ebenso, E. E. (2021). Challenges and advantages of using plant extract as inhibitors in modern corrosion inhibition systems: Recent advancements. Journal of Molecular Liquids, 321, 114666. doi: https://doi.org/10.1016/j.molliq.2020.114666